AIP | Applied Physics Letters

Skyrmion based microwave detectors and harvesting

G. Finocchio, M. Ricci, R. Tomasello, A. Giordano, M. Lanuzza, V. Puliafito, P. Burrascano, B. Azzerboni, and M. Carpentieri

Citation: Applied Physics Letters **107**, 262401 (2015); doi: 10.1063/1.4938539
View online: http://dx.doi.org/10.1063/1.4938539
View Table of Contents: http://scitation.aip.org/content/aip/journal/apl/107/26?ver=pdfcov
Published by the AIP Publishing

Skyrmion based microwave detectors and harvesting

G. Finocchio,[1] M. Ricci,[2] R. Tomasello,[3] A. Giordano,[1] M. Lanuzza,[3] V. Puliafito,[4] P. Burrascano,[2] B. Azzerboni,[4] and M. Carpentieri[5]
[1]*Department of Mathematical and Computer Sciences, Physical Sciences and Earth Sciences, University of Messina, Viale F. Stagno d'Alcontres 31, 98166 Messina, Italy*
[2]*Department of Engineering, Polo Scientifico Didattico di Terni, University of Perugia, Terni, TR I-50100, Italy*
[3]*Department of Computer Science, Modelling, Electronics and System Science, University of Calabria, via P. Bucci 41C, I-87036 Rende (CS), Italy*
[4]*Department of Engineering, University of Messina, c.da di Dio, I-98166 Messina, Italy*
[5]*Department of Electrical and Information Engineering, Politecnico di Bari, via E. Orabona 4, I-70125 Bari, Italy*

(Received 29 September 2015; accepted 11 December 2015; published online 28 December 2015)

Magnetic skyrmions are topologically protected states that are very promising for the design of the next generation of ultra-low-power electronic devices. In this letter, we propose a magnetic tunnel junction based spin-transfer torque diode with a magnetic skyrmion as ground state and a perpendicular polarizer patterned as nano-contact for a local injection of the current. The key result is the possibility to achieve sensitivities (i.e., detection voltage over input microwave power) larger than 2000 V/W for optimized contact diameters. We also pointed out that large enough voltage controlled magnetocrystalline anisotropy could significantly improve the sensitivity. Our results can be very useful for the identification of a class of spin-torque diodes with a non-uniform ground state and to understand the fundamental physics of the skyrmion dynamical properties. © *2015 AIP Publishing LLC*. [http://dx.doi.org/10.1063/1.4938539]

The spin-transfer torque diode (STD) effect is a rectification effect that converts a microwave current in a dc voltage.[1] The physics at the basis of the STD effect is linked to the excitation of the ferromagnetic resonance (FMR). In particular, for a fixed input frequency, the detection voltage V_{dc} is proportional to the amplitude of the microwave current I_{ac}, to the oscillating magneto-resistance ΔR_s, and to the cosine of the phase difference between the two previous signals Φ_s, $V_{dc} = \frac{1}{2} I_{ac} \Delta R_s \cos(\Phi_s)$. Since its discovery in 2005,[1] due to the low sensitivity equal to 1.4 V/W (rectified voltage over input microwave power), this effect has been used only to estimate the torques in magnetic tunnel junctions (MTJs),[2,3] although specific calculations from Ref. 4 suggested that optimized MTJs should reach sensitivities exceeding 10 000 V/W.

From an experimental point of view, the STD sensitivity has been improved by the simultaneous application of a microwave together with a bias current.[5–7] In this case, an additional component proportional to the dc current can contribute to increase the detection voltage.[8,9] Considering the advances in the design of the MTJs, in terms of tunneling magnetoresistive (TMR) effect and voltage controlled magnetocrystalline anisotropy (VCMA),[10] and the understanding of strong non-linear effects, such as stochastic resonance,[9] non-linear resonance,[6] and injection locking,[7] the sensitivity performance of biased STD has reached values as large as 75 000 V/W.[7] Those results on biased STDs open a path for the design of a generation of high sensitivity microwave detectors. On the other hand, unbiased STDs could be also designed to rectify the microwave power from different energy sources, such as satellite, sound, television, and Wi-Fi signals. The resulting dc voltage could charge a cell phone battery, or supply self-powered sensors as well as other small electronic devices. Therefore, the unbiased STDs can be used for both passive microwave detection and power harvesting functionality. Up to now, unbiased STDs have been designed with a uniform ground state and, thanks to the use of both VCMA and spin-transfer torque, a sensitivity of 900 V/W has been measured.[7,10]

Very recently, the stabilization of Néel skyrmions at room temperature has been demonstrated by several groups independently.[11,12] This experimental milestone in the development of ultralow-power devices has motivated the study presented in this letter. We report the results of micromagnetic simulations of STDs where a Néel skyrmion is the magnetic ground state of the free layer. We have considered the diode effect of the skyrmion based STD as response to a microwave current locally injected into the ferromagnet via a nano-contact.

The key quantitative result of this letter is the prediction of sensitivities reaching 2000 V/W at zero field, zero bias current, and low input microwave power ($<1.0\,\mu$W). Our findings are interesting from a technological point of view, in fact skyrmion based STD can be the basis for the design of passive nano-contact microwave detectors and resonant energy harvesting.[13,14] The last part of this work shows the effect of VCMA on the dynamical response of the skyrmion.

We have studied an MTJ (see sketch in Fig. 1), with a circular cross section of diameter $l = 100$ nm. The stack is composed of an iron-rich free layer (0.8 nm) and an MgO spacer with on top a nano-contact of CoFeB acting as current polarizer of diameter $d_C < l$. The system is designed in order that the interfacial perpendicular anisotropy (IPA), due to the electrostatic interaction between the Fe of CoFeB and the O

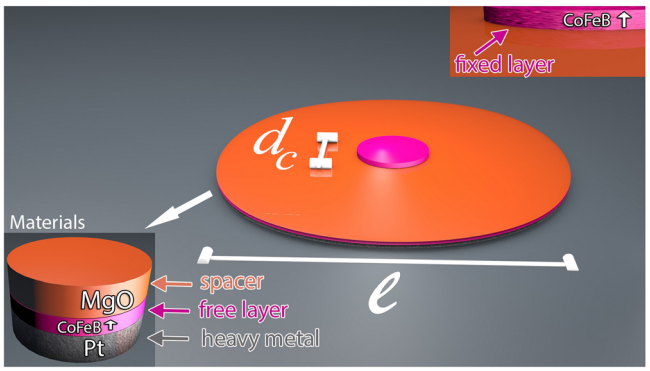

FIG. 1. Sketch of the device under investigation. The extended CoFeB acts as free layer, while the top nano-contact made by CoFeB is the current polarizer (d_C is the contact diameter, $l = 100$ nm). The Pt layer is necessary to introduce the *i*-DMI.

of MgO, is large enough to induce an out of plane easy axis (z-axis) in both ferromagnets.[15] Furthermore, the free layer is coupled to a Pt layer to introduce in its energy landscape an additional degree of freedom due to the interfacial Dzyaloshinskii-Moriya Interaction (*i*-DMI) given by

$$\varepsilon_{DMI} = 2D[m_z \nabla \cdot \mathbf{m} - (\mathbf{m} \cdot \nabla) m_z], \tag{1}$$

where $\mathbf{m}$ is the normalized magnetization vector of the free layer and m_z is its z-component.[16] Basically, the effective field of the free layer takes into account, together with the standard micromagnetic contributions of the exchange and the self-magnetostatic fields, the IPA and the *i*-DMI fields. All the results discussed in this letter are achieved at zero external field. The main simulation parameters are saturation magnetization $M_S = 0.9$ MA/m, Gilbert damping $\alpha_G = 0.03$, and exchange constant $A = 20$ pJ/m. We have performed micromagnetic simulations based on the Landau-Lifshitz-Gilbert (LLG) equation to study the stability and the dynamical response of a single Néel skyrmion as a function of the IPA (k_U represents the IPA constant) and of the *i*-DMI parameter D (see Refs. 17 and 18 for a complete numerical description of the model).

The inset of Fig. 2(a) shows a snapshot of a skyrmion (the arrows refer to the in-plane component of the magnetization, while the color is linked to its out-of-plane component—blue negative and red positive) as ground state of the free layer, where also its diameter d_{SK} is indicated (the radius is calculated as the distance from the geometrical center of the skyrmion, where the out-of-plane component of the magnetization m_Z is -1, to the region where $m_Z = 0$). The main panel of Fig. 2(a) shows the profile of m_Z as computed by considering the section AA′. The negative region coincides with the skyrmion core, while the non-monotonic behavior near the edges is due to the boundary conditions in presence of the *i*-DMI $\frac{d\mathbf{m}}{dn} = \frac{1}{\xi}(\hat{z} \times \mathbf{n}) \times \mathbf{m}$ (where $\xi = \frac{2A}{D}$ is a characteristic length in presence of DMI and $\mathbf{n}$ is the direction normal to the surface).[19] For the nucleation of the skyrmion, we apply a localized dc spin-polarized current following the same procedure described in Ref. 20, finding that the nucleation in a time smaller than 5 ns is achieved with bias current $J = 30$ MA/cm^2.

Figures 2(b) and 2(c) show the skyrmion diameter d_{SK} as a function of D for two values of $k_U = 0.8$ and 0.9 MJ/m^3 and as a function of k_U for $D = 3.0$ and 3.5 mJ/m^2, respectively. In our study, we have used DMI parameters larger than the one estimated in *state of the art* of materials (> 2.0 mJ/m^2 for a ferromagnetic thickness of 0.8 nm).[21–23] However, *ab initio* computations have predicted values of D close to 3.0 mJ/m^2 for Pt/Co bilayers.[24] In addition, this choice can permit to have a comparison with previous numerical studies.[25] The fixed layer diameter d_C, which also corresponds to the nano-contact size, has been chosen to be comparable or larger than the skyrmion diameter. This aspect is important to design the skyrmion based microwave detector in order to optimize its sensitivity as it will be discussed below. To study the microwave dynamical properties, we have considered both the Slonczewski and the field-like torque as additional terms to the LLG equation

$$\frac{g\,|\mu_B|J}{|e|\gamma_0\, M_s^2 t}\, g_T(\mathbf{m}, \mathbf{m_p}) \Big[\mathbf{m} \times (\mathbf{m} \times \mathbf{m_p}) - q(V)(\mathbf{m} \times \mathbf{m_p})\Big], \tag{2}$$

where g is the gyromagnetic splitting factor, γ_0 is the gyromagnetic ratio, μ_B is the Bohr magneton, $q(V)$ is a term which takes into account the voltage-dependence of the field like torque (see Refs. 26 and 27 for more numerical details), $J = J_M \sin(\omega t)$ is the microwave current density, t is the thickness of the free layer, e is the electron charge, and $\mathbf{m_p}$ is the normalized magnetization of the polarizer fixed along the positive z-axis. $g_T(\mathbf{m}, \mathbf{m_p}) = 2\eta_T(1 + \eta_T{}^2 \mathbf{m} \cdot \mathbf{m_p})^{-1}$ is the polarization function.[28,29] We have used for the spin-polarization η_T the value 0.66.[2] Numerically, the resistance of the device R is given by $R = R_P + (R_{AP} - R_P)(1 - \langle m_z \rangle)$ being the polarizer aligned along the positive z-axis, while R_{AP} and R_P are the resistances in the antiparallel and parallel state, respectively. Within the approximation that the direction of the magnetization changes sharply from down (-1) to up ($+1$) when moving across a skyrmion, R can be estimated directly from the skyrmion diameter d_{SK} as follow:

$$R = \begin{cases} R_P\left(1 - \dfrac{d_{SK}^2}{d_C^2}\right) + R_{AP}\dfrac{d_{SK}^2}{d_C^2}; & d_{SK} < d_C \\ R_{AP}; & d_{SK} \geq d_C, \end{cases} \tag{3}$$

for $d_{SK} < d_C$ the left (right) contribution is related to the micromagnetic cells below the nanocontact where $m_z > 0$ ($m_z < 0$).

To characterize the dynamical response of the STD, we have also used the detection sensitivity ε computed as the ratio between the detection voltage and the input microwave power (P_{in}) $\varepsilon = \frac{V_{dc}}{P_{in}}$. P_{in} is the active power delivered to the MTJ, computed as $P_{in} = 0.5 J_M^2 S^2 R$, being R the static resistance (see Eq. (3)) and S the contact area.

Figures 3(a) and 3(b) show the STD response as a function of the microwave frequency ($d_C = 40$ nm) achieved for $J_M = 3$ MA/cm^2, in (a) $k_U = 0.8$ MJ/m^3 is maintained fixed while $D = 2.5$, 3.0, 3.5, and 4.0 mJ/m^2, and in (b) $D = 3.0$ mJ/m^2 while k_U changes from 0.7 MJ/m^3 to 0.9 MJ/m^3. The skyrmion response is mainly characterized by the excitation of a breathing mode of its core, with a preserved radial symmetry, similarly to the uniform breathing mode described

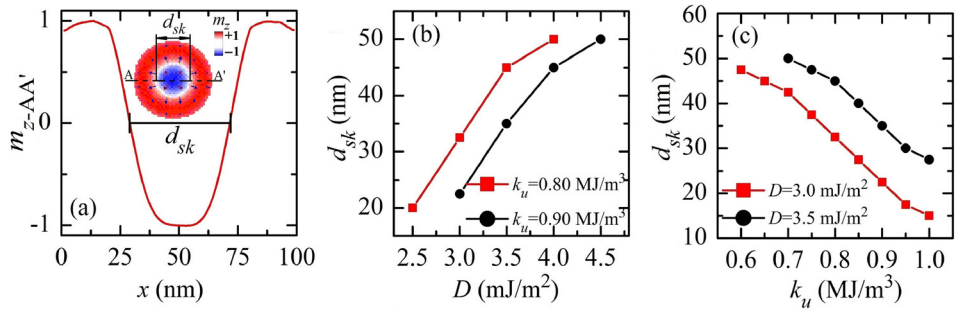

FIG. 2. (a) Profile of the out-of-plane component of the magnetization corresponding to the section AA′, as indicated in the inset. d_{sk} represents the skyrmion diameter. Inset: example of a snapshot of a Néel skyrmion stabilized by the *i*-DMI, where the arrows indicate the in-plane component of the magnetization while the colors are linked to the out-of-plane component (blue negative, red positive). (b) and (c) Skyrmion diameter as computed by means of micromagnetic simulations (the radius is computed as the distance from the geometrical center of the skyrmion, where $m_Z = -1$, to the region where $m_Z = 0$). Skyrmion diameter (b) as a function of D for $k_U = 0.8$ and 0.9 MJ/m^3 and (c) as a function of k_U for $D = 3.0$ and 3.5 mJ/m^2.

in literature.[25,30,31] The weak sinusoidal microwave current (quasi-monochromatic signal) excites the uniform breathing mode, being the skyrmion response in a quasi-linear regime. This mode induces a resistance oscillation of amplitude ΔR_s linked to the minimum and maximum skyrmion core diameter $d_{SK\text{-}min}$ and $d_{SK\text{-}max}$ and given by

$$\Delta R_S = \begin{cases} (R_{AP} - R_P)\dfrac{d^2_{SK-\max} - d^2_{SK-\min}}{d_C^2} & d_{SK-\max} < d_C \\ (R_{AP} - R_P)\left(1 - \dfrac{d^2_{SK-\min}}{d_C^2}\right) & d_{SK-\max} \geq d_C, \end{cases} \quad (4)$$

ΔR_S is as larger as $d^2_{SK-\min} - > 0$ and $d_{SK-\max} - > d_C$. Moreover, as expected, the ferromagnetic resonance frequency does not change with the contact diameter d_C (not shown), being linked to the excitation of the uniform breathing mode of the skyrmion. An example of the time and space domain evolution of the skyrmion core at the resonance frequency $f = 4.6$ GHz ($k_U = 0.8$ MJ/m^3 and $D = 3.0$ mJ/m^2) is shown in Ref. 32.

The FMR frequencies as a function of D for different k_U are summarized in Fig. 3(c). This non-monotonic trend can be attributed to a different effect of the confining force (self-magnetostatic field) on the skyrmion uniform breathing mode. To qualitatively understand this behavior, we refer to the concept of critical D (D_{crit}) introduced in Ref. 19. For extended ferromagnets, when D is below D_{crit}, the confining force is negligible, whereas for D near or above D_{crit}, the confining force plays a crucial role in fixing the skyrmion size. We argue that this fact gives rise to the different slopes of the FMR frequency vs D for our system. Those arguments are confirmed by micromagnetic simulations performed for devices with diameter $l = 75$ nm and 150 nm ($k_U = 0.80$ MJ/m^3) and displayed in Fig. 3(d). For $l = 75$ nm, the confining force acts on the skyrmion also at small D giving rise to a monotonic FMR frequency vs D curve. On the other hand, for

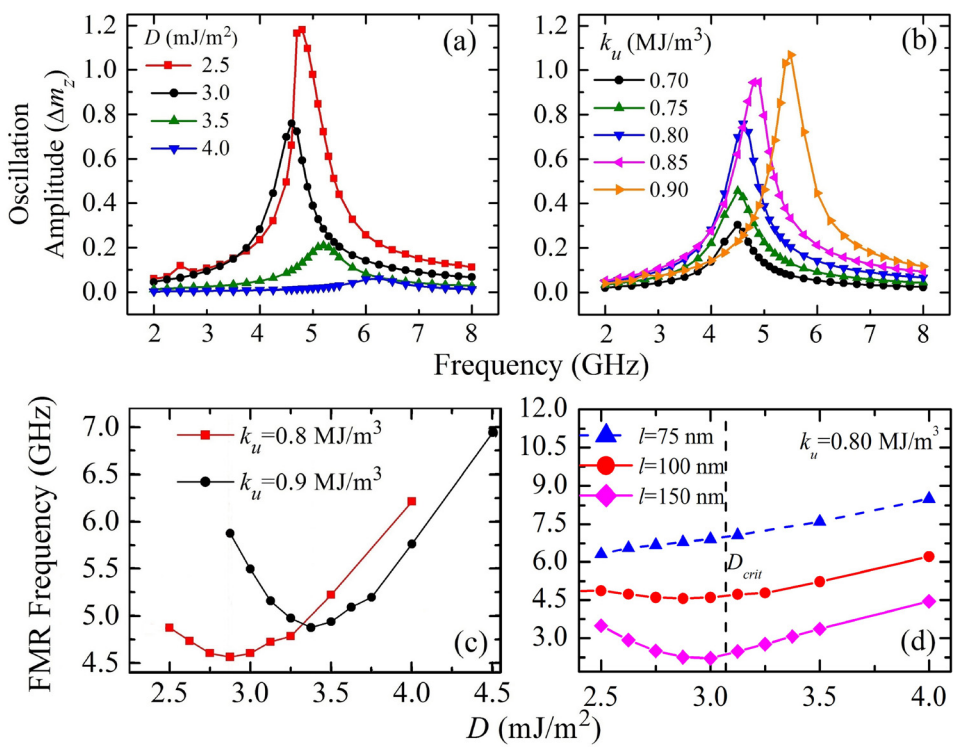

FIG. 3. (a) STD response as a function of D for $k_U = 0.8$ MJ/m^3. (b) STD response as a function of k_U for $D = 3.0$ mJ/m^2. (c) FMR frequency as a function of D for two different values of k_U as indicated in the panel. (d) FMR frequency as a function of D ($k_U = 0.8$ MJ/m^3) for three different values of the cross section diameter $l = 75$, 100, and 150 nm with the indication of the critical DMI parameter D_{crit}.

$l = 150$ nm the non-monotonic trend is exhibited again and the minimum moves towards $D = D_{crit} = 3.07\,\mathrm{mJ/m^2}$, as expected.

To compare the skyrmion-based STD to the *state-of-the-art* MTJ-based STDs, we have performed a systematic study of the sensitivity computed at the FMR frequency as a function of the d_C ($30\,\mathrm{nm} < d_C < 60\,\mathrm{nm}$). All the data discussed below are obtained for $k_U = 0.8\,\mathrm{MJ/m^3}$ and $D = 3.0\,\mathrm{mJ/m^2}$; however, qualitative similar results have been achieved for $k_U = 0.9\,\mathrm{MJ/m^3}$ and $D = 2.5$ and $3.5\,\mathrm{mJ/m^2}$.

Fig. 4(a) summarizes the sensitivities computed for four different current amplitudes $J_M = 1-4\,\mathrm{MA/cm^2}$ maintained constant at different d_C ($R_{AP} = 1.5\,\mathrm{k\Omega}$ and $R_P = 1\,\mathrm{k\Omega}$).[33] One key finding is the existence of an optimal contact size where the sensitivity exhibits a maximum value. This result can be qualitatively understood as follow. For a fixed skyrmion ground state, the change in the d_C introduces a change in the microwave power (both static resistance R and contact cross section depend on d_C). Fig. 4(b) displays the detection voltage and the input microwave power as a function of the contact size for $J_M = 1\,\mathrm{MA/cm^2}$. As can be observed, both the detection voltage and the input microwave power increase as a function of d_C. Their ratio determines the optimal d_C, as reported in Fig. 4(a). In particular, the key condition to be fulfilled is

$$\frac{d\varepsilon}{d(d_c)} = \frac{1}{P_{in}^2}\left(P_{in}\frac{dV_{dc}}{d(d_c)} - V_{dc}\frac{dP_{in}}{d(d_c)}\right) = 0, \qquad (5)$$

which should be solved numerically. The second result is the prediction, for an optimal configuration, of sensitivities of the order of 2000 V/W, which are larger than the ones of *state of the art* unbiased MTJ-based STDs around 900 V/W.[7,10]

Fig. 4(c) summarizes the sensitivities computed as a function of the d_C for different values of the microwave power. Those computations also show the existence of an optimal contact, which coincides with the maximum of the detection voltage, as summarized in Fig. 4(d). In fact, for the last computational framework, the Eq. (6) holds $\frac{d\varepsilon}{d(d_c)} = \frac{dV_{dc}}{d(d_c)} = 0$. As can be observed, the two maxima differ by less than 5 nm (compare Figs. 4(a) and 4(c)).

The last part of the letter investigates a possible contribution of the VCMA to the sensitivity of skyrmion based STDs.[34] We have implemented this contribution as an additive field to the effective field as $H_{VCMA} = \Delta H_{VCMA}\sin(\omega t)$ applied along the out-of-plane direction.[35] In CoFeB/MgO/CoFeB stacks, the VCMA has been already used to demonstrate the electrical field assisted switching[36] and to improve the sensitivity of unbiased STDs.[7,10] We have performed an ideal numerical experiment considering the optimal scenario of Fig. 4(a) ($d_C = 40\,\mathrm{nm}$, FMR frequency $\approx 4.6\,\mathrm{GHz}$). At $J_M = 0\,\mathrm{MA/cm^2}$, the H_{VCMA} drives an oscillating z-component of the magnetization whose amplitude as a function of ΔH_{VCMA} is displayed in Fig. 5(a). The key difference with parametric resonance is the absence of a threshold value for the excitation of dynamics. In other words, the VCMA acts on a skyrmion state as linear excitation.[35] Fig. 5(b) shows the sensitivities as a function of the ΔH_{VCMA} for $J_M = 1$ and $2\,\mathrm{MA/cm^2}$. The minimum in the sensitivity around $\Delta H_{VCMA} = 4\,\mathrm{mT}$ can be explained by the change in the phase Φ_s (see Fig. 5(c)). While the amplitude of the ΔR_S monotonically increases with the ΔH_{VCMA}, the Φ_s is non-monotonic: firstly it decreases up to a minimum value at $\Delta H_{VCMA} = 4\,\mathrm{mT}$ ($\Phi_s = 0.66\pi$ for $J_M = 1\,\mathrm{MA/cm^2}$) and then increases. An in-depth analysis of the micromagnetic configurations shows that at low ΔH_{VCMA} both $d_{SK-\min}$ and $d_{SK-\max}$ change ($d_{SK-\min}$ decreases and $d_{SK-\max}$ increases). On the other hand, as the ΔH_{VCMA} increases, it exists a critical value at which the $d_{SK-\max}$ saturates to d_C, while $d_{SK-\min}$ will continue to decrease. In this way, ΔR_S (see Eq. (4)) and, consequently, V_{dc} increase, proving that the presence of a large enough VCMA effect can significantly improve the sensitivity of the skyrmion based STD.

To estimate the VCMA contribution, we consider the optimal case of Fig. 4(a), $J_M = 1\,\mathrm{MA/cm^2}$ and a typical

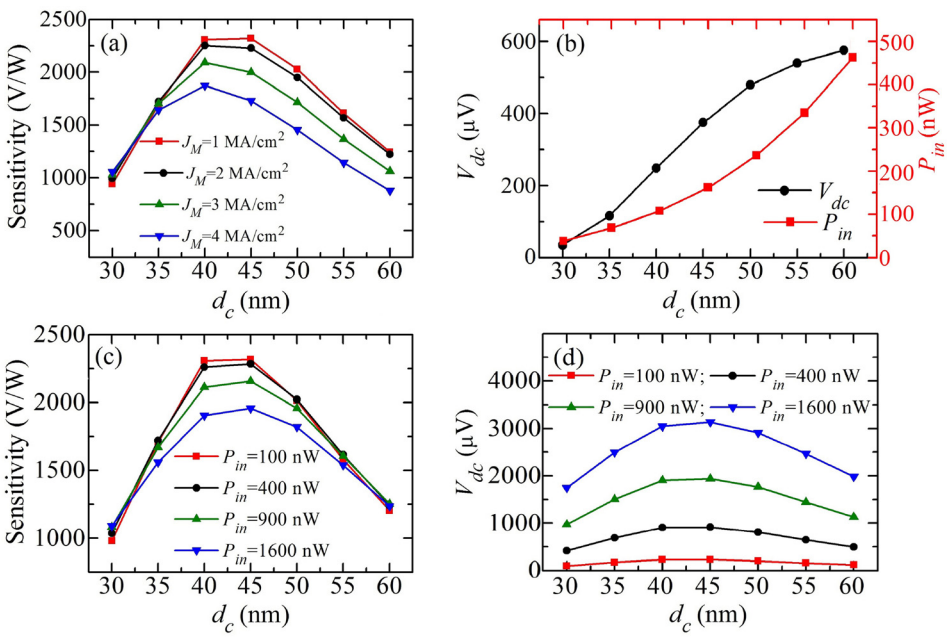

FIG. 4. (a) Sensitivity as a function of the contact diameter for different amplitudes of the microwave current as indicated in the main panel. (b) Detection voltage and microwave power as a function of the contact diameter for $J_M = 1\,\mathrm{MA/cm^2}$. (c) Sensitivity as a function of the contact diameter for different microwave powers as indicated in the main panel. In both (a) and (c), an optimal contact diameter corresponding to a maximum in the sensitivity can be observed. (d) Detection voltage as a function of the contact diameter for different microwave powers. All the data reported in this figure are obtained for $k_U = 0.8\,\mathrm{MJ/m^3}$ and $D = 3.0\,\mathrm{mJ/m^2}$.

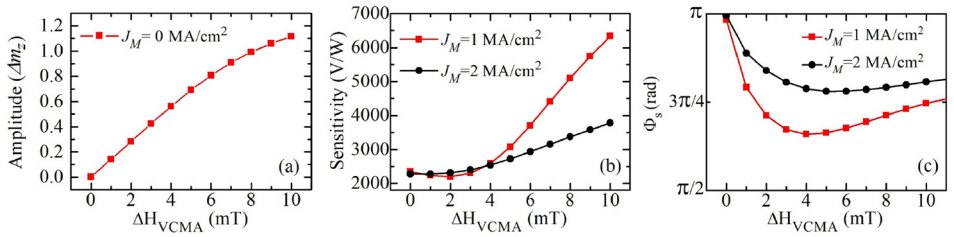

FIG. 5. (a) Amplitude of the z-component of the magnetization driven by ΔH_{VCMA} at $J_M = 0\,\mathrm{MA/cm^2}$; (b) sensitivity as a function of the ΔH_{VCMA}, considering the optimal contact diameter of Fig. 4(a) ($d_C = 40\,\mathrm{nm}$), computed for $J_M = 1$ and $2\,\mathrm{MA/cm^2}$. (c) Phase shift Φ_s as a function of ΔH_{VCMA} for the same microwave currents amplitudes of (b).

experimental VCMA value of 60 mT/V.[10] However, by using *state of the art* values of VCMA, the $\Delta H_{VCMA} \approx 1\,\mathrm{mT}$ would result negligible giving rise to a negligible effect in our devices.

In summary, we have proposed a zero field and an unbiased skyrmion based STD for passive microwave detection and energy harvesting application. The skyrmion is stabilized by the *i*-DMI and when it is supplied by a microwave spin current with perpendicular polarization, a breathing mode is excited. The change in the size of the skyrmion is converted to a change of the TMR signal, which gives rise to a detection voltage. We have pointed out that sensitivities as large as 2000 V/W can be achieved for optimized contact diameter. Our results open a path for fundamental physics in understanding the skyrmion dynamical properties and for the design of STD with a non-uniform ground state.

This work was supported by the project PRIN2010ECA8P3 from Italian MIUR. The work of G.F. and M.C. was also supported by the bilateral agreement Italy-Turkey project (Code B52I14002910005) "Nanoscale magnetic devices based on the coupling of Spintronics and Spinorbitronics." The authors thank Domenico Romolo for the support in making Figure 1. M.R. and P.B. acknowledge financial support from Fondazione CARIT - Progetto Sensori Spintronici.

[1]A. A. Tulapurkar, Y. Suzuki, A. Fukushima, H. Kubota, H. Maehara, K. Tsunekawa, D. D. Djayaprawira, N. Watanabe, and S. Yuasa, Nature **438**, 339–342 (2005).
[2]J. C. Sankey, Y.-T. Cui, J. Z. Sun, J. C. Slonczewski, R. A. Buhrman, and D. C. Ralph, Nat. Phys. **4**, 67–71 (2008).
[3]H. Kubota, A. Fukushima, K. Yakushiji, T. Nagahama, S. Yuasa, K. Ando, H. Maehara, Y. Nagamine, K. Tsunekawa, D. D. Djayaprawira *et al.*, Nat. Phys. **4**, 37–41 (2008).
[4]C. Wang, Y.-T. Cui, J. Z. Sun, J. A. Katine, R. A. Buhrman, and D. C. Ralph, J. Appl. Phys. **106**, 053905 (2009).
[5]X. Cheng, C. T. Boone, J. Zhu, and I. N. Krivorotov, Phys. Rev. Lett. **105**, 047202 (2010).
[6]S. Miwa, S. Ishibashi, H. Tomita, T. Nozaki, E. Tamura, K. Ando, N. Mizuochi, T. Saruya, H. Kubota, K. Yakushiji *et al.*, Nat. Mater. **13**, 50–56 (2014).
[7]B. Fang, M. Carpentieri, X. Hao, H. Jiang, J. A. Katine, I. N. Krivorotov, B. Ocker, J. Langer, K. L. Wang, B. Zhang *et al.*, e-print arXiv:1410.4958.
[8]G. Finocchio, I. N. Krivorotov, X. Cheng, L. Torres, and B. Azzerboni, Phys. Rev. B **83**, 134402 (2011).
[9]X. Cheng, J. A. Katine, G. Rowlands, and I. N. Krivorotov, Appl. Phys. Lett. **103**, 082402 (2013).
[10]J. Zhu, J. A. Katine, G. E. Rowlands, Y.-J. Chen, Z. Duan, J. G. Alzate, P. Upadhyaya, J. Langer, P. K. Amiri, K. L. Wang *et al.*, Phys. Rev. Lett. **108**, 197203 (2012).
[11]C. Moreau-Luchaire, C. Moutafis, N. Reyren, J. Sampaio, N. Van Horne, C. A. F. Vaz, K. Bouzehouane, K. Garcia, C. Deranlot, P. Warnicke *et al.*. e-print arXiv:1502.07853.
[12]S. Woo, K. Litzius, B. Krüger, M.-Y. Im, L. Caretta, K. Richter, M. Mann, A. Krone, R. Reeve, M. Weigand *et al.*, e-print arXiv:1502.07376.
[13]S. Hemour and K. Wu, Proc. IEEE **102**, 1668–1691 (2015).
[14]A. M. Hawkes, A. R. Katko, and S. A. Cummer, Appl. Phys. Lett. **103**, 163901 (2013).
[15]S. Ikeda, K. Miura, H. Yamamoto, K. Mizunuma, H. D. Gan, M. Endo, S. Kanai, J. Hayakawa, F. Matsukura, and H. Ohno, Nat. Mater. **9**, 721–724 (2010).
[16]T. Moriya, Phys. Rev. Lett. **4**, 228 (1960).
[17]R. Tomasello, E. Martinez, R. Zivieri, L. Torres, M. Carpentieri, and G. Finocchio, Sci. Rep. **4**, 6784 (2014).
[18]R. Tomasello, M. Carpentieri, and G. Finocchio, J. Appl. Phys. **115**, 17C730 (2014).
[19]S. Rohart and A. Thiaville, Phys. Rev. B **88**, 184422 (2013).
[20]J. Sampaio, V. Cros, S. Rohart, A. Thiaville, and A. Fert, Nat. Nanotechnol. **8**, 839 (2013).
[21]M. Belmeguenai, J.-P. Adam, Y. Roussigné, S. Eimer, T. Devolder, J.-V. Kim, S. M. Cherif, A. Stashkevich, and A. Thiaville, Phys. Rev. B **91**, 180405(R) (2015).
[22]J. Cho, N.-H. Kim, S. Lee, J.-S. Kim, R. Lavrijsen, A. Solignac, Y. Yin, D.-S. Han, N. J. J. van Hoof, H. J. M. Swagten *et al.*, Nat. Commun. **6**, 7635 (2015).
[23]S. Pizzini, J. Vogel, S. Rohart, L. D. Buda-Prejbeanu, E. Jué, O. Boulle, I. M. Miron, C. K. Safeer, S. Auffret, G. Gaudin *et al.*, Phys. Rev. Lett. **113**, 047203 (2014).
[24]H. Yang, A. Thiaville, S. Rohart, A. Fert, and M. Chshiev, e-print arXiv:1501.05511v1.
[25]J.-V. Kim, F. Garcia-Sanchez, J. Sampaio, C. Moreau-Luchaire, V. Cros, and A. Fert, Phys. Rev. B **90**, 064410 (2014).
[26]G. Finocchio, B. Azzerboni, G. D. Fuchs, R. A. Buhrman, and L. Torres, J. Appl. Phys. **101**, 063914 (2007).
[27]Z. Zeng, G. Finocchio, B. Zhang, P. K. Amiri, J. A. Katine, I. N. Krivorotov, Y. Huai, J. Langer, B. Azzerboni, K. L. Wang *et al.*, Sci. Rep. **3**, 1426 (2013).
[28]J. C. Slonczewski, Phys. Rev. B **71**, 024411 (2005); J. C. Slonczewski and J. Z. Sun, J. Magn. Magn. Mater. **310**, 169–175 (2007).
[29]A. Giordano, G. Finocchio, L. Torres, M. Carpentieri, and B. Azzerboni, J. Appl. Phys. **111**, 07D112 (2012).
[30]S.-Z. Lin, C. D. Batista, and A. Saxena, Phys. Rev. B **89**, 024415 (2014).
[31]C. Schutte and M. Garst, Phys. Rev. B **90**, 094423 (2014).
[32]See supplementary material at http://dx.doi.org/10.1063/1.4938539 for a video of the spin-dynamics at resonant frequency.
[33]H. Meng, R. Sbiaa, M. A. K. Akhtar, R. S. Liu, V. B. Naik, and C. C. Wang, Appl. Phys. Lett. **100**, 122405 (2012).
[34]T. Maruyama, Y. Shiota, T. Nozaki, K. Ohta, N. Toda, M. Mizuguchi, A. A. Tulapurkar, T. Shinjo, M. Shiraishi, S. Mizukami *et al.*, Nat. Nanotechnol. **4**, 158–161 (2009).
[35]R. Verba, V. Tiberkevich, I. Krivorotov, and A. Slavin, Phys. Rev. Appl. **1**, 044006 (2014).
[36]W. G. Wang, M. Li, S. Hageman, and C. L. Chien, Nat. Mater. **11**, 64–68 (2012).